

WAVE PROPAGATION IN A FLUID-FILLED FRACTURE—AN EXPERIMENTAL STUDY

by

X.M. Tang, and C.H. Cheng

Earth Resources Laboratory
Department of Earth, Atmospheric, and Planetary Sciences
Massachusetts Institute of Technology
Cambridge, MA 02139

ABSTRACT

A laboratory experimental study has been carried out to investigate the mode trapping characteristics of a fluid-filled fracture between two elastic solids. Using a small circular cylindrical receiver of 2.7 mm diameter, we were able to measure the wave motion directly inside a 2.8 mm thick fracture and to obtain array data for the propagating waves. The data was processed using Prony's method to give velocity of the wave modes as a function of frequency. The experimental results agree with the theoretical predictions quite well. Specifically, in a "hard" (aluminum) fracture where the shear velocity of the solid is greater than the fluid velocity, four normal modes were detected in the frequency range up to 2.4 MHz. Whereas in a "soft" (lucite) fracture where the shear velocity is smaller than the fluid velocity, four leaky-P modes were detected in the same frequency range. In both cases, a fundamental mode analogous to Stoneley waves in a borehole was detected. In particular, the velocity of this mode approaches zero in the low frequency limit, as indicated by the theory and confirmed by the experiment in a low frequency range down to 25 kHz.

INTRODUCTION

The dynamic wave motion in a fluid-filled fracture is of considerable geophysical importance. For example, in VSP surveys, seismic waves may excite such a wave motion in a borehole fracture, generating tube waves in the borehole (Beydoun et al., 1985), while in acoustic logging measurements, this wave motion can be generated in a borehole fracture by the passing borehole acoustic waves. Recently, such a wave motion has been related to the interpretation of volcanic tremors (Chouet, 1986; Ferrazzini and Aki, 1987; Chouet, 1988). Because this wave motion is such an interesting phenomenon, it has attracted quite a few studies. Chouet (1986) and Chouet and Julian (1985) have numerically analyzed the fluid motion in a finite crack and its coupling

with the surrounding solid. Ferrazzini and Aki (1987) have analytically studied the wave modes in a fluid-filled fracture. Although a fracture modeled as a fluid layer between two elastic half-spaces behaves essentially like a wave guide, and is in many ways analogous to a fluid-filled borehole (Paillet and White, 1982), it exhibits an unusual behavior; both the Chouet (1986) and Ferrazzini and Aki (1987) studies predict the existence of slow waves, whose velocity, unlike that of their borehole counterpart tube waves, approaches zero as the wavelength goes to infinity. The wave modes existing in a borehole environment have long been observed both in the laboratory (Chen, 1982, 1988) and in the field (Williams et al., 1984), whereas the observation of waves in a fluid-filled fracture has not yet been reported. The objective of the study is to give an experimental confirmation of the theory on wave propagation in a fluid-filled fracture.

THEORY

The wave modes existing in a fluid layer sandwiched between two elastic solids are given by the following dispersion equation (Ferrazzini and Aki, 1987; Paillet and White, 1982)

$$\cot \left(\frac{h\omega}{2v} \sqrt{\frac{v^2}{v_f^2} - 1} \right) = \frac{\rho_s v_s^4 \sqrt{\frac{v^2}{v_f^2} - 1}}{\rho_f v^4 \sqrt{1 - \frac{v^2}{v_p^2}}} \left[\left(2 - \frac{v^2}{v_s^2} \right)^2 - 4 \sqrt{1 - \frac{v^2}{v_s^2}} \sqrt{1 - \frac{v^2}{v_p^2}} \right] \quad (1)$$

where v is the phase velocity of the modes, v_f , v_p , and v_s are the acoustic velocity in fluid, compressional and shear velocities in the solid, respectively. ρ_f and ρ_s are density of fluid and solid, respectively. h is the fracture aperture, ω is the angular frequency, and \cot represents the cotangent function. In cases where the elastic solid is hard ($v_p > v_s > v_f$), a number of normal modes analogous to pseudo-Rayleigh waves in a borehole exist with different cut-off frequencies. Starting from the shear wave velocity of the solid at the cut-off frequencies, the wave velocities of these modes approach the fluid velocity at high frequencies (see Paillet and White, 1982; Ferrazzini and Aki, 1987). The cases where the solid is soft ($v_p > v_f > v_s$) have not attracted much attention. As we will show later, this situation is also analogous to that of a fluid-filled borehole surrounded by a soft formation as studied by Paillet and Cheng (1986) in which a number of leaky-P modes exist with different cut-off frequencies. Starting from the compressional velocity of the solid at the cut-off frequencies, the velocities of the leaky-P modes approach the fluid velocity as frequency increases. In both hard and soft situations, a fundamental mode exists for all frequencies. This mode is comparable to the borehole tube wave mode studied by Biot (1952) and Cheng and Toksöz (1981). At high frequencies both the fracture and the borehole modes propagate at the velocity of the Stoneley wave along the fluid-solid interface. (For this reason, this fundamental mode will be termed "Stoneley" in the following text.) However,

there is a fundamental difference between the two types of wave modes in that the velocity of the fracture mode goes to zero at very low frequencies while the velocity of the borehole tube mode approaches a finite value. Consequently, slow waves exist in a fluid-filled fracture. This has been demonstrated by Chouet (1986) in his finite difference modeling. The theoretical predictions will be illustrated as we compare them to the laboratory experimental results.

EXPERIMENTAL PROCEDURE

The ideal situation for detecting wave motion in a fracture is to measure the waves directly inside the fracture. In the ultrasonic experiment, care must be taken to ensure that the fracture aperture lies in the range of ultrasonic wavelengths, so that the effects of these waves are easily measurable. For this purpose, the fracture aperture cannot be too large and a small receiver is needed. We use a cylindrical receiver of 2.7 mm in diameter and 29 mm in length. This receiver is made of piezoelectric materials. The fracture aperture is thus chosen as $h = 2.8$ mm. It should be noted that Eq. (1) is derived assuming plane wave propagation in an infinitely long fracture. In reality, however, it is difficult to generate plane waves because of the finite size of a transducer source. But it is relatively easy to produce cylindrical waves. As shown in Figure 1, a cylindrical fracture is simulated by a gap between the smooth ends of two cylinders. A cylindrical hydrophone source of 0.97 cm diameter and 300 kHz center frequency is placed at the center of the fracture through the central hole of the two cylinder blocks. The diameter of the hole is 1 cm. For this experimental geometry, the wave propagation in the fracture is cylindrically symmetric. It can be shown that the same dispersion equation as Eq. (1) can be derived for the radial propagation. For the elastic solid, we use aluminum to simulate "hard" solid and lucite "soft" solid. Their acoustic properties are given in Table I. The lucite cylinder is 15 cm in diameter and 15 cm in height. The aluminum cylinder is 20 cm in diameter and 15 cm in height. During the experiment, the assembly designed in Figure 1 is submerged in a water tank. The receiver is initially placed with its full length (29 mm) into the fracture (Figure 1). When the received waveform is digitized at a receiver position, the receiver is automatically moved to the next position at a 1 mm step by a step motor controller. With 25 receiver positions, array data for the propagating waves are obtained. We apply Prony's method (Lang et al., 1986; Ellefsen et al., 1987) to process the data. Assuming the homogeneity of the formation and fluid along the array data, this method of array processing involves changing the data from the time domain to the frequency domain by applying a fast Fourier transform to each trace and then estimating the amplitude and wavenumber (phase) for each propagating wave mode at every frequency using the method of least squares. The velocity estimate is quite accurate when waves have high amplitude. However, as encountered in every array processing technique, the quality of the estimate will be degraded when waves have low

amplitude because of the noise in the data. Due to the finite length of our receiver, such effects as reflections from the fracture opening at the outer surface of the cylindrical sample will unavoidably appear in the received waveform. Fortunately, these effects can be discriminated by Prony's method because of their different wavenumbers.

EXPERIMENTAL RESULTS

Figure 2 shows the full waveform data for the aluminum fracture. The waves are somewhat similar to those one would have seen from the well-log data. The small amplitude first arrivals are the compressional head waves. Following them are the strongly dispersive normal modes (analogous to pseudo-Rayleigh waves in a borehole). Then come the large amplitude arrivals. They are the Stoneley mode similar to tube waves in a borehole situation. One also notices strongly reflected waves from the fracture opening at the outer surface of the sample because of the large acoustic impedance contrast between water and aluminum. Figure 3 shows the velocities obtained from the array data. The theoretical dispersion curves calculated using Eq. (1) and parameters in Table I are also plotted versus the experimental results. As can be seen from this figure, in the frequency range of 0-2.4 MHz, we essentially pick up five wave modes, four normal modes and the Stoneley. The Stoneley velocities are well picked up because these waves have large amplitude and therefore large signal to noise ratios. The normal mode velocities show some scatters around the theoretical curves because these waves have much smaller signal to noise ratios than those of the Stoneley. Despite the scatters in the experimental results, the theory and experiment agree fairly well. Figure 4 shows the full waveform data for the lucite fracture. Three signals are apparent in this figure. The first arrivals move out approximately at the compressional velocity of lucite (2700 m/s). They are the leaky-P wave trains. The second high frequency arrivals are "water" waves, with velocity of about 1460 m/s. The last arrivals are considerably slower, at a velocity of about 1000 m/s. (Because the acoustic impedance contrast between water and lucite is much smaller than that of the aluminum case, one can barely see strong reflections from the fracture opening, as we have seen in Figure 2.) It is interesting to note that similar wave types have been observed in a soft formation borehole model experiment (Chen, 1988; Figure 2). The velocities obtained using Prony's method are given in Figure 5. The theoretical dispersion curves calculated using Eq. (1) and the parameters given in Table I are also plotted versus the experimental results. Because the Stoneley energy is mostly within 500 kHz, the experimental results fit the theory very well in this frequency range. Outside this range, the theory and experiment fit reasonably well, though with some scatters. Apart from the Stoneley, we pick up four leaky-P modes. The water arrivals are the superposition of the high frequency branches of the leaky-P modes. For the leaky-P modes, the experimental results are biased from the theory, particularly in the second and third modes. This could be due to the fact that the hydrophone source sketched in Figure 1 was not

quite symmetric with respect to the center plane of the fracture. The wave emissions of the borehole source from both sides of the fracture were not equal. They could easily penetrate the soft formation and generate some antisymmetric modes (Ferrazzini and Aki, 1987) to interfere with the symmetric leaky-P modes. Whereas in the aluminum fracture case, these extra emissions could barely penetrate the formation because of the large acoustic impedance contrast between water and aluminum. In spite of the discrepancy in the second and third modes, the separation of velocities into individual modes is clearly apparent and the general agreement of the experiment with the theory is quite good. To show the low frequency behavior of velocity dispersion of the Stoneley waves in a fracture, we plot the theoretical and experimental results for the lucite fracture in a lower frequency range of 0-200 kHz (Figure 6). As predicted by the theory, the experimental velocity data decreases as frequency goes to zero, indicating the existence of slow waves at low frequencies. Due to the ultrasonic source used in the laboratory, we were unable to generate low frequency signals. However, in the case of a volcanic tremor as discussed by Ferrazzini and Aki (1987) and Chouet (1986, 1988), the magma activity in the volcanic chamber may act as a low frequency source to excite slow waves in a magma-filled crack, generating the low frequency events as observed by Sassa (1935).

CONCLUSIONS

In this study, we have experimentally investigated the wave motion in a fluid-filled fracture. We have verified that in a hard fracture a number of pseudo-Rayleigh type modes exist and in a soft fracture a number of leaky-P modes exist, and that in both cases a Stoneley type mode exists for all frequencies. In particular, our experimental results indicate that the velocity of this Stoneley mode decreases with decreasing frequency, thus giving an experimental proof to the existence of slow fracture waves as predicted by Chouet (1986) and Ferrazzini and Aki (1987).

ACKNOWLEDGEMENTS

We would like to thank Karl J. Ellefsen for providing us with his program for the array data processing. This research was supported by the Full Waveform Acoustic Logging Consortium at M.I.T. and by Department of Energy grant No. DE-FG02-86ER13636.

REFERENCES

- Beydoun, W.B., Cheng C.H., and Toksöz, M.N., Detection of open fractures with vertical seismic profiling, *J. Geophys. Res.*, *90*, 4557-4566, 1985.
- Biot, M.A., Propagation of elastic waves in a cylindrical bore containing a fluid; *J. Appl. Phys.*, *23*, 977-1005, 1952.
- Chen, S.T., The full acoustic wavetrain in a laboratory model of a borehole; *Geophysics*, *47*, 1512-1520, 1982.
- Chen, S.T., Shear-wave logging with dipole sources; *Geophysics*, *53*, 659-667, 1988.
- Cheng, C.H., and Toksöz, M.N., Elastic wave propagation in a fluid-filled borehole and synthetic acoustic logs; *Geophysics*, *46*, 1042-1053, 1981.
- Chouet, B., Dynamics of a fluid driven crack in three dimensions by the finite difference method; *J. Geophys. Res.*, *90*, 13967-13992, 1986.
- Chouet, B., Resonance of a fluid-driven crack: Radiation properties and implication for the source of long-period events and harmonic tremor; *J. Geophys. Res.*, *93*, 4375-4400, 1988.
- Chouet, B., and Julian, B.R., Dynamics of an expanding fluid-filled crack; *J. Geophys. Res.*, *90*, 11184-11198, 1985.
- Ellefsen, K.J., Cheng, C.H., and Duckworth, G.L., Estimating phase velocity and attenuation of guided waves in acoustic logging data; *Expd. Abst., Soc. Expl. Geophys., 57th Ann. Int. Mtg. and Exposition*, New Orleans, Louisiana, 1987.
- Ferrazzini, V., and Aki, K., Slow waves trapped in a fluid-filled infinite crack: implication for volcanic tremor; *J. Geophys. Res.*, *92*, 9215-9223, 1987.
- Lang, S.W., Kurkjian, A.L., McCellan, J.H., Morris, C.F., and Parks, T.W., Estimating slowness dispersion from arrays of sonic logging data, *Geophysics*, *52*, 530-544, 1987.
- Paillet, F.L., and White, J.E., Acoustic modes of propagation in the borehole and their relationship to rock properties; *Geophysics*, *47*, 1215-1228, 1982.
- Paillet, F.L., and Cheng, C.H., A numerical investigation of head waves and leaky modes in fluid-filled boreholes, *Geophysics*, *51*, 1438-1449, 1986.
- Sassa, K., Volcanic micro-tremors and eruption-earthquakes; *Mem. Coll. Sci. Univ. Kyoto, Ser. A.*, *18*, 255-293, 1935.

Williams, D.M., Zamanek, J., Angona, F.A., Dennis, C.L., and Caldwell, R.L., The long space acoustic logging tool; *Trans. SPWLA 25th Ann. Logging Symp.*, Paper T, 1984.

Medium	ρ (g/cm ³)	v_p (m/sec)	v_s (m/sec)
Aluminum	2.7	6410	3180
Lucite	1.2	2700	1300
Water	1.0	1460	0

Table I: Density ρ , compressional velocity v_p , and shear velocity v_s of the fluid and solid used in the measurement.

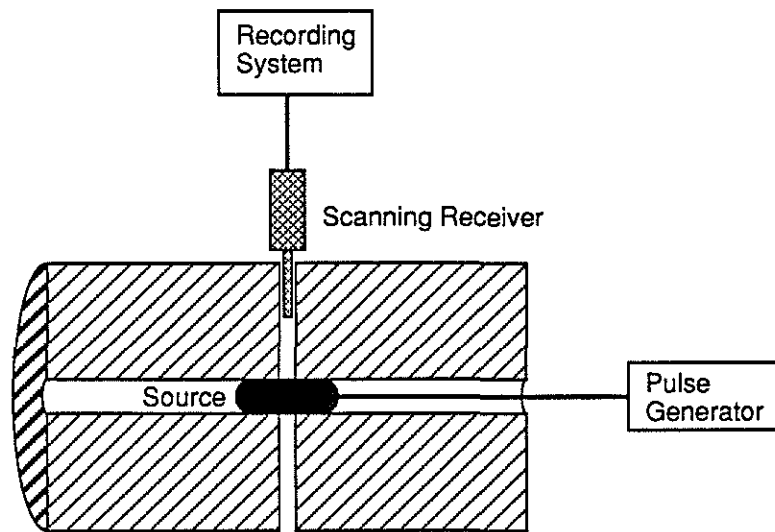


Figure 1: Experimental design for measuring wave propagation in a fluid-filled fracture. The fracture is simulated by a gap between the ends of two solid cylinders. A hydrophone source is at the center of the fracture while a small receiver is placed into the fracture to measure the waves.

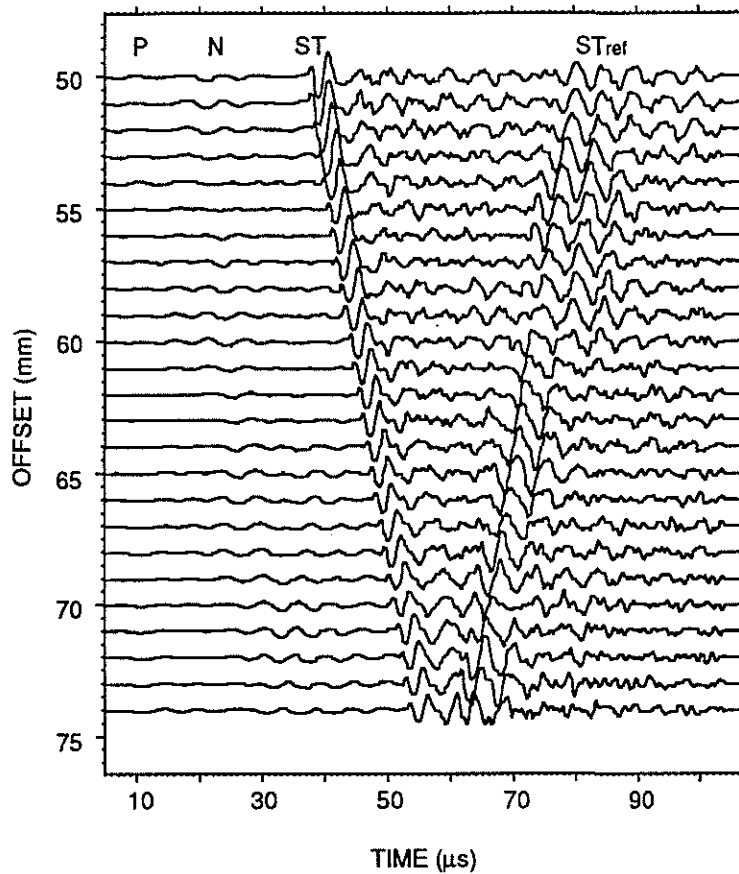


Figure 2: Full waveform data received in the aluminum fracture at varying source-receiver distances. From the top, the distance is increased 1 mm per trace. The time sampling interval is $0.2 \mu s$. The labels are: P – compressional head waves, N – normal modes, ST – Stoneley, and ST_{ref} – reflected Stoneley waves from the fracture opening at the outer surface of the sample.

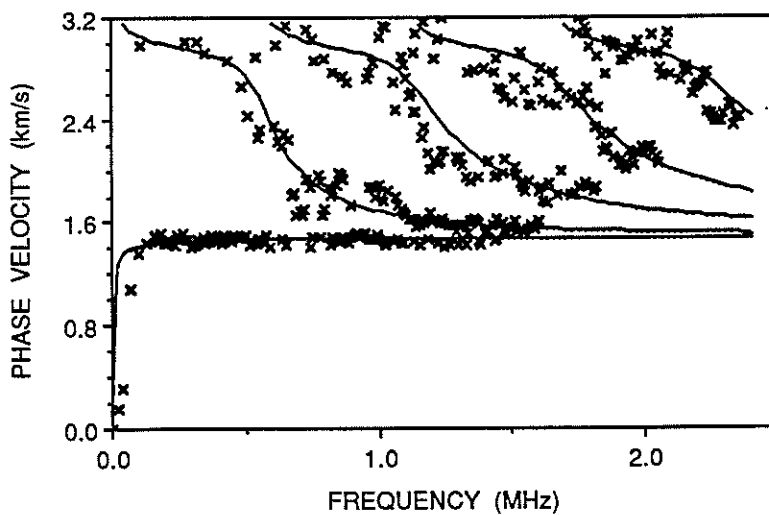


Figure 3: Comparison of theoretical and experimental wave mode velocities as a function of frequency for the aluminum fracture. The theoretical dispersion curves are calculated using Eq. (1) and the parameters given in Table I. The experimental results (indicated by crosses) are obtained by applying Prony's method to the array data shown in Figure 2.

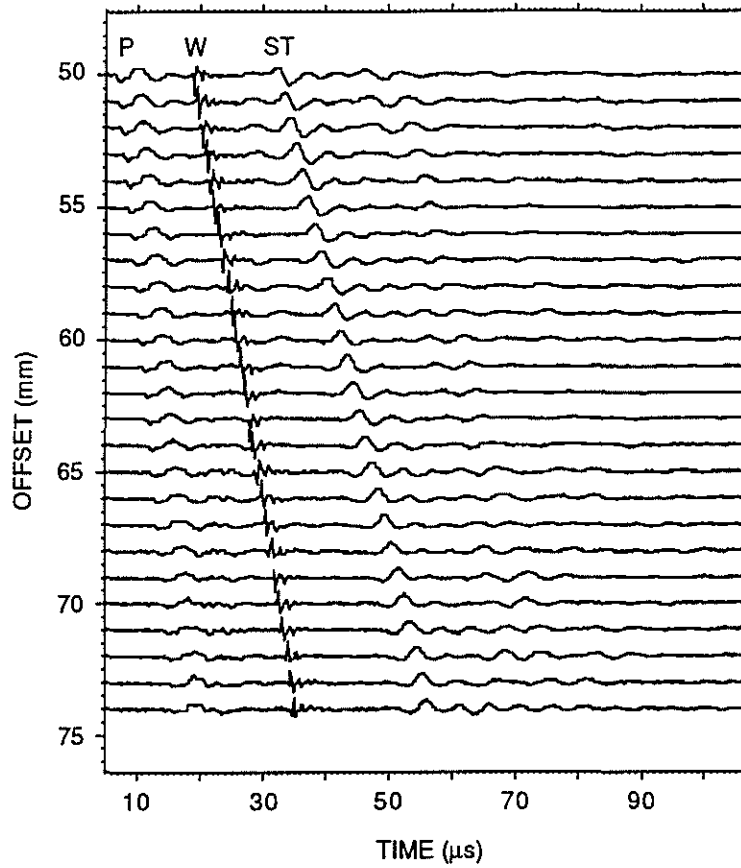


Figure 4: Full waveform array data received in the lucite fracture at varying source-receiver distances. The distance between adjacent traces is 1 mm. The time sampling interval is $0.2 \mu s$. The labels are: P – leaky-P waves, W – water waves, and ST – Stoneley waves.

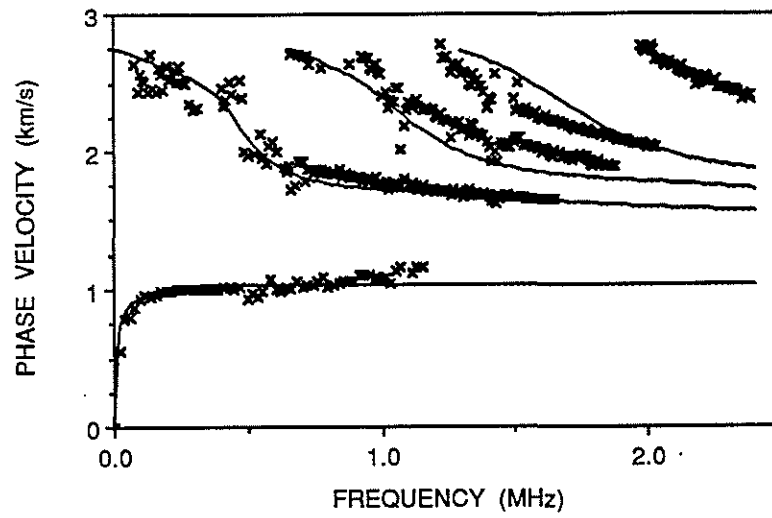


Figure 5: Comparison of the theoretical and experimental wave mode velocities as a function of frequency for the lucite fracture. Note that the pseudo-Rayleigh type of modes in Figure 3 become leaky-P modes in the “soft” fracture case.

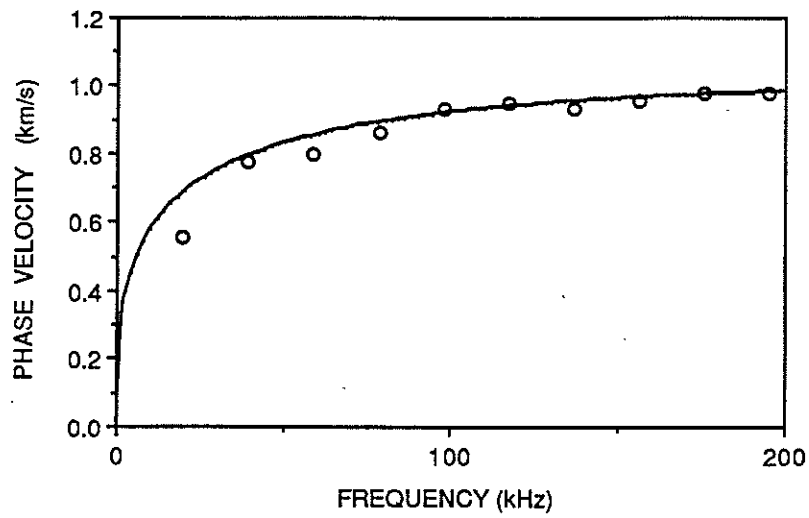


Figure 6: Comparison of theoretical and experimental Stoneley mode velocities in a lower frequency range (0–200 kHz). As predicted by the theory (thick curve), the experimental velocity (data points) decreases as the frequency approaches zero.